

## Supplementary Information

### Experimental and Theoretical Photoluminescence Studies in Nucleic Acid Assembled Gold-Upconverting Nanoparticle Clusters

Liangcan He<sup>‡,1</sup> Chenchen Mao<sup>‡,2</sup> Suehyun Cho,<sup>2</sup> Ke Ma,<sup>1</sup> Weixian Xi,<sup>1</sup> Christopher N. Bowman,<sup>1,3</sup> Wounjhang Park,<sup>2,3</sup> \* Jennifer N. Cha<sup>1,3\*</sup>

<sup>1</sup>Department of Chemical and Biological Engineering, <sup>2</sup>Department of Electrical, Computer and Energy Engineering, <sup>3</sup>Materials Science and Engineering, University of Colorado, Boulder

\*To whom correspondence should be addressed to: won.park@colorado.edu, jennifer.cha@colorado.edu

<sup>‡</sup>These authors contributed equally to this work.

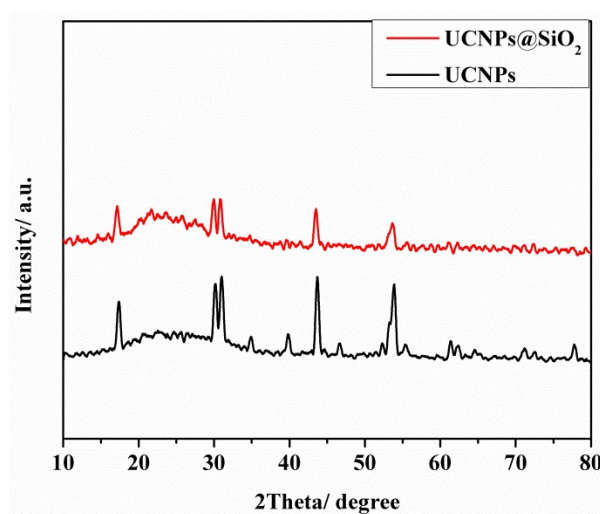


**Figure S1.** X-ray powder diffraction (XRD) patterns of the UCNPs and silica coated UCNPs.

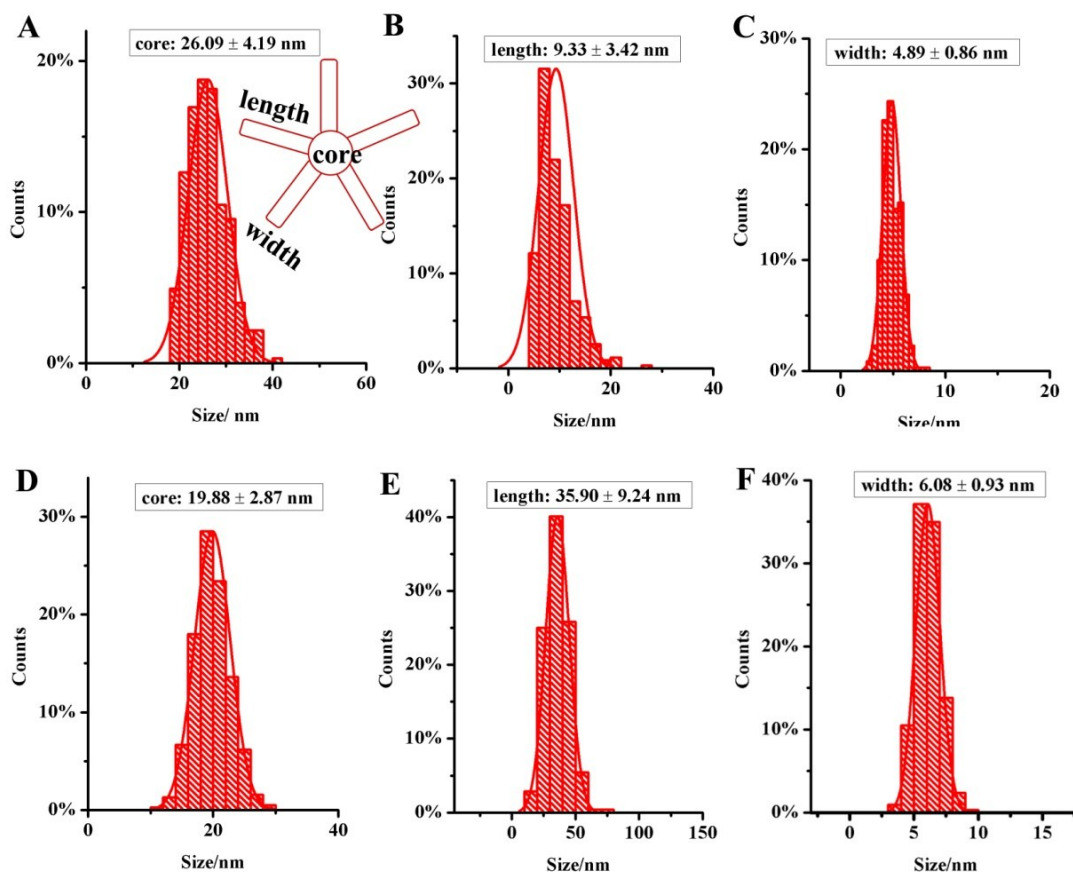


**Figure S2.** Dimension parameters of the (A, B and C) AuNSs with 700nm plasmon and (D, E and F) AuNSs showing 980nm plasmon.

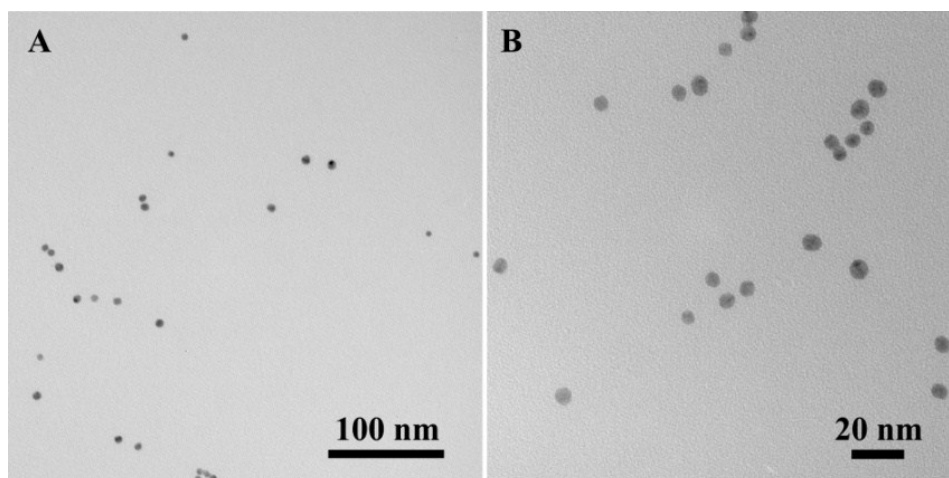


**Figure S3.** (A) TEM images and (B) magnified TEM images of AuNPs (absorption peak: 520nm).

For 5 nm AuNPs, its extinction coefficient is  $9.696 \times 10^6 \text{ M}^{-1}\text{cm}^{-1}$ .

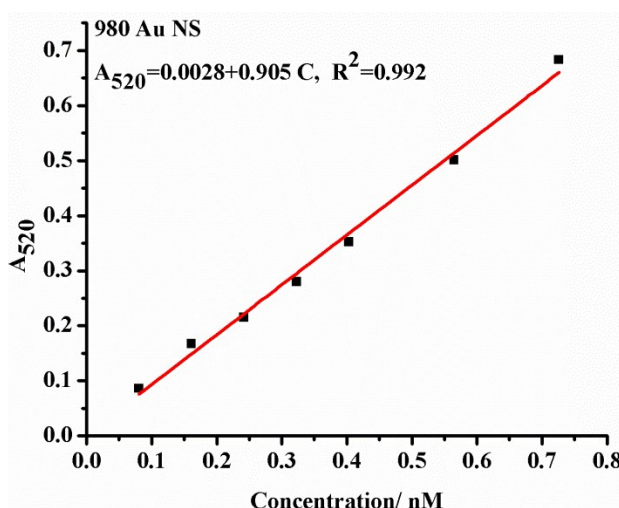


**Figure S4.** Concentration-absorption standard curve of the AuNSs showing 980nm plasmon in aqueous solution.

Because AuNSs possess cores whose dimensions are  $\sim 19.9\text{nm}$  which are very close to 20 nm, the core contributes predominantly to the 520nm plasmon peak while the branches of the stars correspond to the plasmon position and intensity in the NIR region<sup>[1]</sup>. It is therefore reasonable to calculate the AuNSs concentration using the absorption peak of the core at 520nm. The 20 nm AuNPs extinction coefficient ( $9.406 \times 10^8 \text{ M}^{-1}\text{cm}^{-1}$ ) was used to calculate the concentration of the AuNSs.

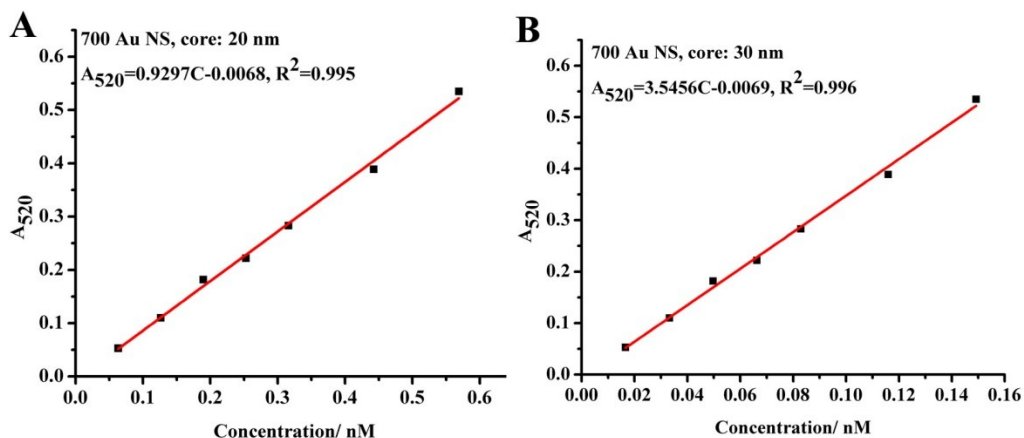


**Figure S5.** Concentration-absorption standard curves of the AuNSs showing plasmon at ~700nm (A) according to 20 nm AuNPs cores (B) according to 30 nm AuNPs cores (30 nm AuNPs extinction coefficient:  $3.585 \times 10^9 \text{ M}^{-1}\text{cm}^{-1}$ ).

The concentration of 26.09 nm 700 AuNSs was calculated according to curve A (Figure S5 A) and curve B (Figure S5 B), then taking the mean value as the 700 AuNSs concentration.

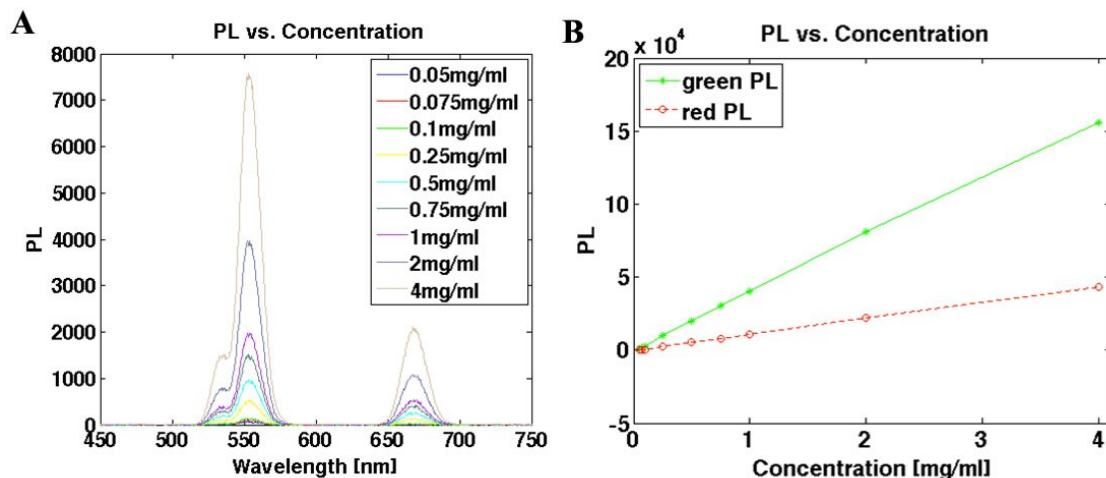


**Figure S6.** UCNPs concentration-PL intensity standard curve.

**Calculation of UCNPs concentration:** Then densities of  $\beta\text{-NaYF}_4$ ,  $\text{NaYbF}_4$  and  $\text{NaErF}_4$  are 4.312, 6.413 and 6.140  $\text{g/cm}^3$  according to standard JCPDS card of each materials, respectively<sup>[2]</sup>.

$$m(\text{UCNP}) = \rho V = [0.8 \times 4.312 + 0.18 \times 6.413 + 0.02 \times 6.140] \times 4 \times \pi (r)^3 / 3$$

The particle concentration corresponding to 1 mg/mL of 20 nm UCNPs is about 83.95 nM.

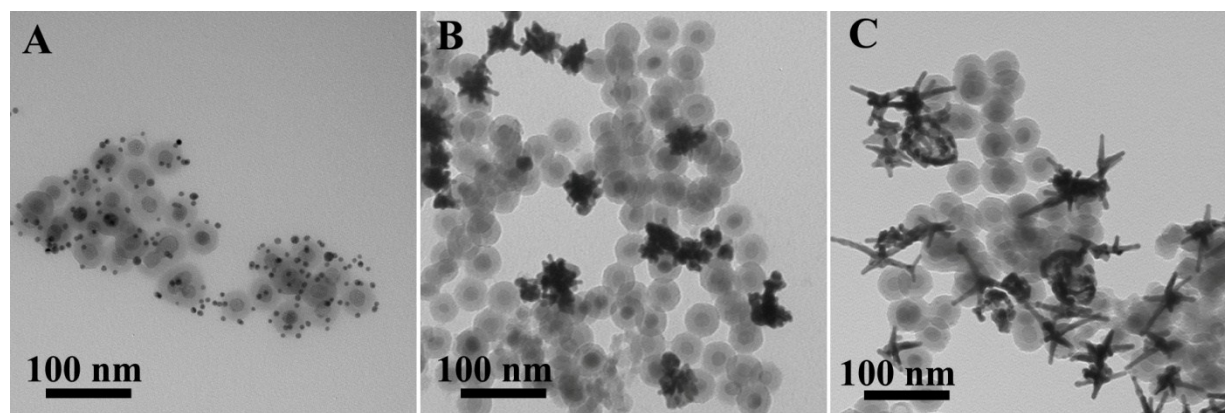


**Figure S7.** TEM images of the Au-UCNP clusters (A) AuNP-UCNP, (B) 700 AuNS-UCNP, (C) 980 AuNS-UCNP. The molar ratios of AuNP:UCNP and AuNS:UCNP used here were 5:1 and 1:1 respectively.

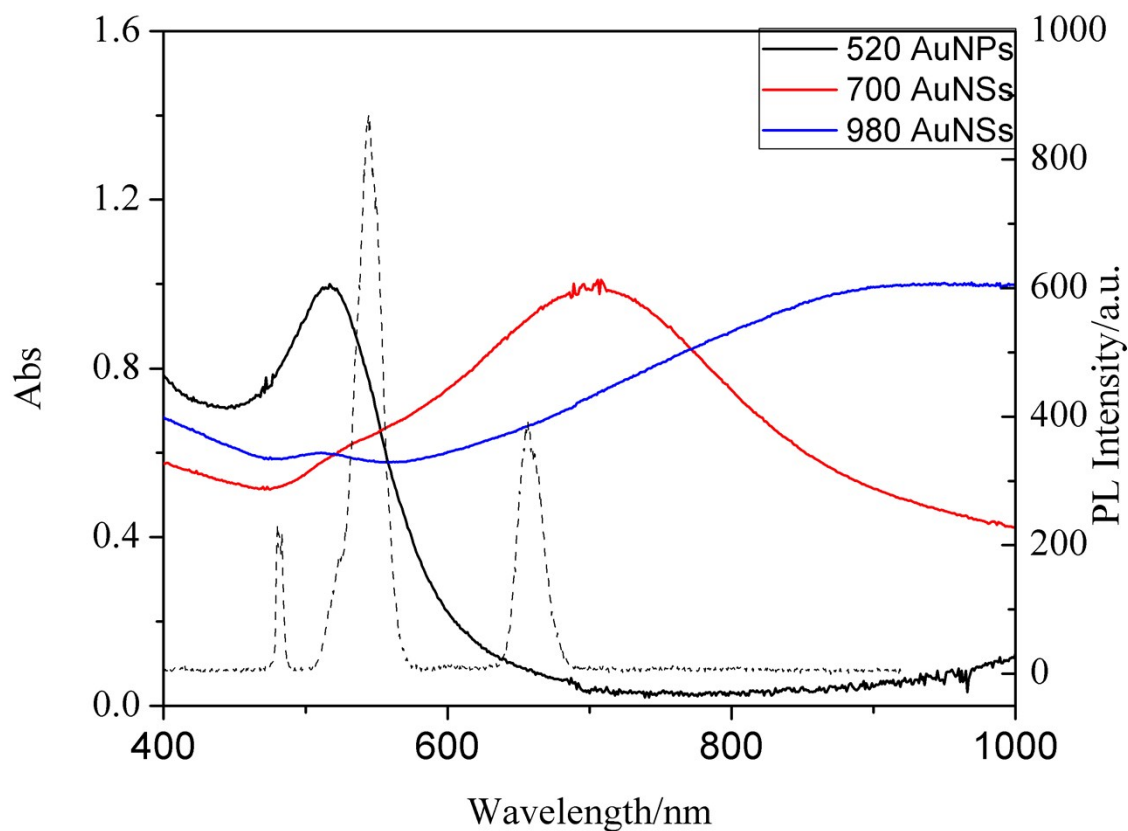


**Figure S8.** Normalized UV-vis spectra of 520 AuNPs, 700 AuNSs and 980 AuNSs. Dotted line corresponding to the upconversion luminescence of the NaYF<sub>4</sub>:Yb/Er UCNPs.

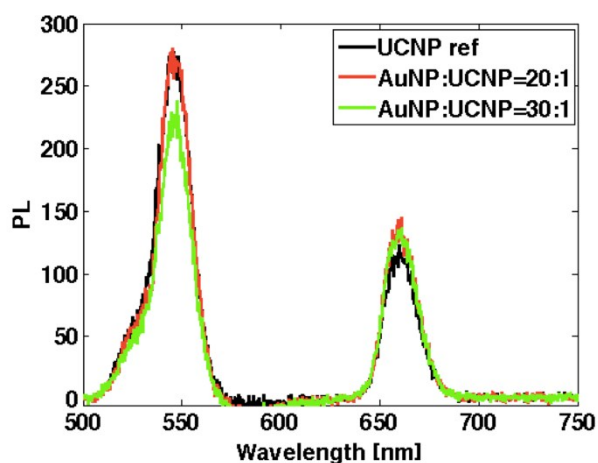


**Figure S9.** Fluorescence spectra of Au-UCNP clusters with higher Au:UCNP ratios.

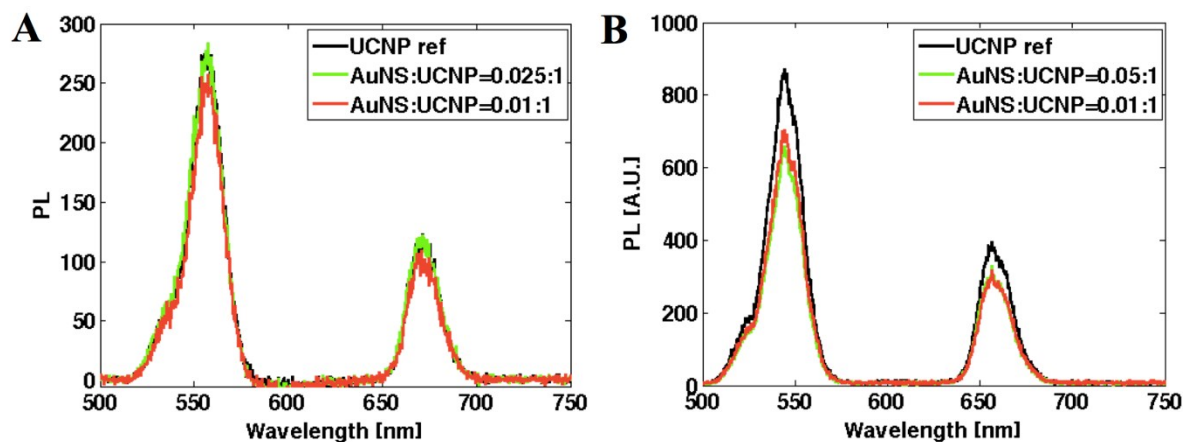


**Figure S10.** Fluorescence spectra of AuNS-UCNP clusters (A: 700 AuNSs; B: 980 AuNS) with lower Au:UCNP ratios.

NS700nm	520 nm	700 nm	
	2.78×10 <sup>-16</sup> m <sup>2</sup>	1.24×10 <sup>-15</sup> m <sup>2</sup>	

NS980nm	520nm	740nm	980nm
	1.15×10 <sup>-16</sup> m <sup>2</sup>	1.60×10 <sup>-16</sup> m <sup>2</sup>	4.14×10 <sup>-16</sup> m <sup>2</sup>

**Table S1.** Extinction cross-section the AuNSs

**Simulation Details:**



To gain quantitative understanding of upconversion enhancement by gold nanostructures, we conducted numerical simulations using the commercial software COMSOL. The geometries used in the simulations are shown in Figure S11 and Figure S12. The exact geometrical parameters were determined by the TEM images (Figure S2). For the AuNPs, the average diameter determined by TEM was used. For AuNSs, we first fixed the number of arms to be 5, the average value obtained from TEM. We then varied the arm length and width within the range observed in TEM to find the geometry that results in the plasmon resonance at 700nm and 980nm. The calculated extinction spectra for the three cases – AuNPs, AuNSs with plasmon resonance at 700nm and AuNSs with plasmon resonance at 980nm – are shown in Figure S13. It should be noted that our samples have wide variations in their sizes and shapes and the experimental data represent ensemble averages of all possible configurations. For this reason, the experimental extinction spectra are significantly more broadened than the simulated spectra. The three geometries shown in Figure S12 should thus be considered as the representative case in each sample.

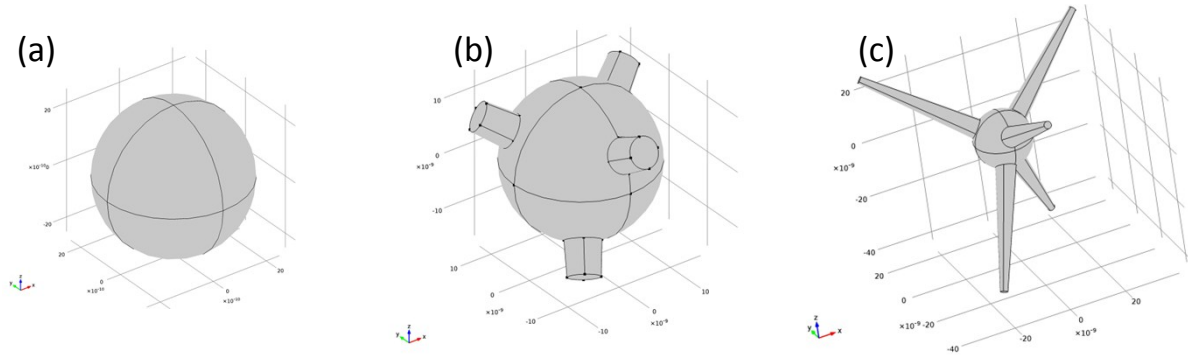


**Figure S11.** The geometries used in the numerical simulations for (a) AuNPs (radius = 2.5 nm), (b) AuNSs with 700nm plasmon resonance (core radius = 13 nm, arm length = 6 nm, arm width is continuously tapered from 5.9 nm at the bottom to 5.2 nm at the top) and (c) AuNSs with 980 nm plasmon resonance (core radius = 10 nm, arm length = 42 nm, arm width is continuously tapered from 6.9 nm at the bottom to 2.5 nm at the top).

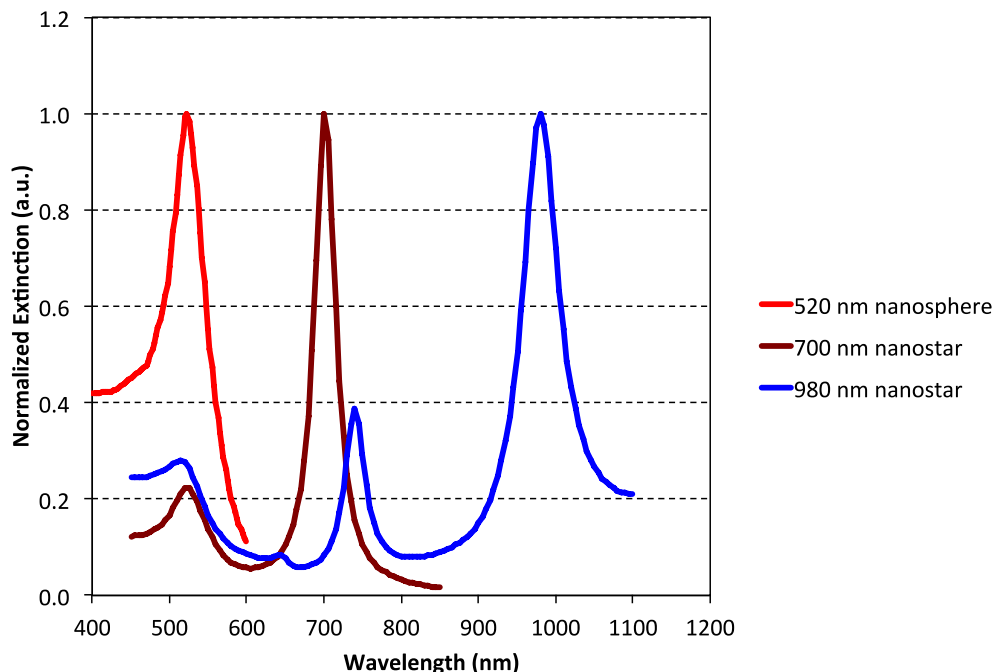


**Figure S12.** Calculated extinction spectra for AuNPs and two AuNSs described in Figure S11.

To estimate the effect of surface plasmon, two simulations were performed. First, the local field amplitude in the vicinity of the gold nanostructure was calculated for a plane wave incidence. The total absorption depends on the local light intensity or  $|E|^2$ . Thus any enhancement or quenching of absorption is given by  $|E/E_0|^2$  where  $E_0$  is the electric field in the absence of gold nanostructure. The electric field patterns calculated at the excitation wavelength of 980nm are shown in Figure 5 (reproduced as Figure S13 below for readability). For AuNPs, thanks to the spherical symmetry, the electric field pattern shows the characteristic dipole pattern for all incident angles and polarizations. For AuNSs, the field pattern depends on the orientation of the NSs relative to the direction of incident light and polarization. However, since the five arms are isotropically placed, the field pattern shows the same general trend where the arm(s) closest to the incident light direction is most strongly excited while the other arms remain relatively cold. Two typical examples are shown in Figure S13(b) and (c).



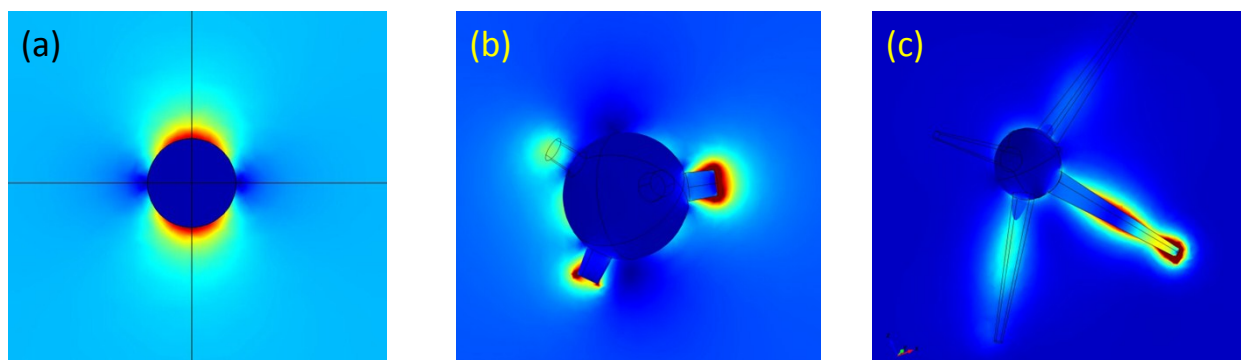


**Figure S13.** Electric field amplitude in the vicinity of (a) AuNPs, (b) AuNSs with 700nm plasmon resonance and (c) AuNSs with 980nm plasmon resonance.

The enhancement factor is dependent on the position. Since our UCNPs have a core diameter of 20 nm and 10 nm silica coating, the maximum and minimum distances to the metal surface available for the optically active ions are 30 and 10 nm, respectively. For AuNPs, the extent of field enhancement is very short and at distances between 10 and 30 nm the field variations were small. The maximum intensity enhancement was 3% and the maximum quenching was 2%. Overall the absorption remained the same with AuNPs. The field patterns for NSs are much more complex and we evaluated the field at various positions around the tip of the arms. For 700nm AuNSs, the intensity enhancement factor,  $|E/E_0|^2$ , varied between 0.60 and 2.00 while it ranged from 0.96 to 1.59 for 980nm AuNSs.

We then conducted emission simulations in which the luminescence from the optically active ion was simulated by a point dipole. The increased local density of states in the vicinity of plasmonic nanostructure could enhance emission rate, a phenomenon known as the Purcell effect. This effect can be numerically evaluated by comparing the radiation rate of the point dipole with and without the gold nanostructure. Once again, for the AuNPs, we only need to consider two polarizations, radial and azimuthal, for the dipole emitter placed at several distances away from the metal surface, thanks to its symmetry. For distances between 10 and 30 nm from the metal surface, the emission enhancement factor stays very close to unity. For AuNSs, many more different positions and polarizations must be considered. We calculated emission enhancement along several different directions from the gold tip at distances between 10 and 30 nm. For 700nm AuNSs, the emission enhancement factor was found to range between 0.3 and 2.8. For 980nm AuNSs, it varied from 0.79 to 1.04.

The total enhancement or quenching of upconverted luminescence can now be obtained by the product of the absorption and emission enhancement factors. To properly represent the experiments where the UCNP and gold nanostructures are randomly coupled together, the total enhancement factors should be evaluated at a variety of positions and averaged. Because of the wide variations in the exact configurations of UCNP and gold nanostructures, it is impossible to precisely reproduce the experimental results. Nevertheless, the simulations provide theoretical basis for the anticipated enhancements. For AuNPs, absorption exhibited small enhancement and emission small quenching. Overall, small enhancement in upconverted

luminescence is expected. The 700nm AuNSs exhibits large enhancement at some positions and strong quenching at others. The volume where quenching is expected is larger than the volume exhibiting enhancement. Thus, an ensemble average over randomly conjugated complexes is likely to exhibit small quenching. The 980nm AuNSs is similar except that the variations in absorption and emission enhancement factors are smaller than the 700nm AuNSs. Once again, small net quenching is expected, as observed experimentally.

Selected simulation results are summarized in the tables below.

AuNP	Excitation enhancement	Emission enhancement		Total enhancement	
		Green	Red	Green	Red
d=10nm	1.001	0.987	0.991	0.988	0.992
d=20nm	1.001	0.991	0.990	0.992	0.991
d=30nm	1.001	0.990	0.991	0.991	0.992

**Table S2.** Emission, excitation and total enhancement of upconversion at various distances from the AuNPs surface

AuNS700nm		Excitation	Emission		Total enhancement	
		980nm	Green	Red	Green	Red
Tip Case 1	d=10nm	1.997	0.949	0.776	1.895	1.550
	d=20nm	1.231	0.991	0.908	1.220	1.118
	d=30nm	1.1025	0.990	0.956	1.091	1.054
Tip Case 2	d=10nm	0.598	1.844	2.075	1.103	1.241
	d=20nm	0.64	1.366	1.185	0.874	0.758
	d=30nm	0.846	1.137	0.945	0.962	0.799

**Table S3.** Emission, excitation and total enhancement of upconversion at various directions from the tip of one of the NSs arms for 700nm AuNSs. The distance from the gold surface was varied from 10 to 30 nm. Tip case 1 represents the direction along the arm and tip case 2 represents the direction perpendicular to the arm. Tip case 2 contains results from several different azimuthal directions.

AuNS980nm		Excitation	Emission		Total enhancement	
		980nm	Green	Red	Green	Red
Tip Case 1	d=10nm	1.588	0.958	0.914	1.521	1.451
	d=20nm	0.980	0.979	0.971	0.959	0.952
	d=30nm	0.960	0.986	0.983	0.947	0.944
Tip Case 2	d=10nm	1.435	1.001	1.031	1.436	1.479
	d=20nm	1.017	0.997	0.999	1.014	1.016
	d=30nm	1.036	0.998	0.997	1.034	1.033

**Table S4.** Emission, excitation and total enhancement of upconversion at various distances and directions from the tip of one of the NSs arms for 980nm AuNSs. The distance from the gold surface was varied from 10 to 30 nm. Tip case 1 represents the direction along the arm and tip case 2 represents the direction perpendicular to the arm. Tip case 2 contains results from several different azimuthal directions.

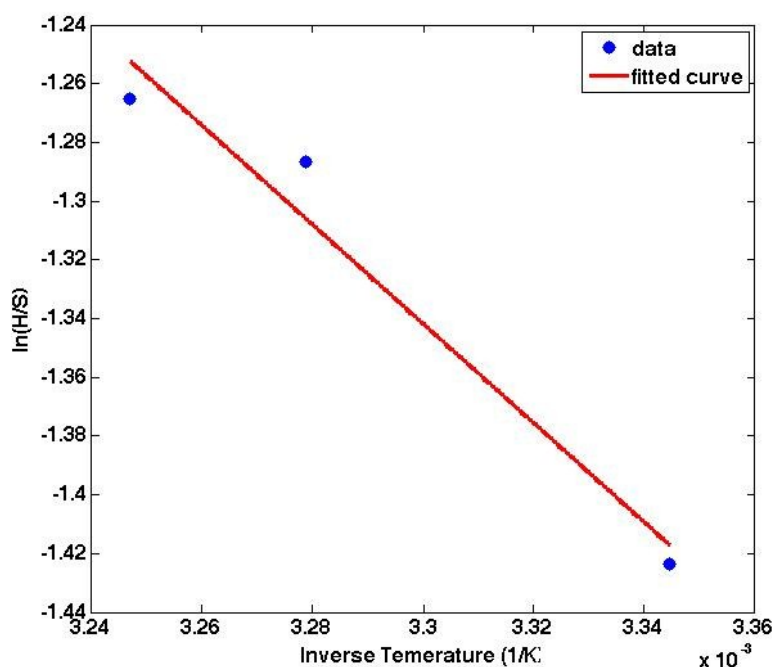


**Figure S14.** Temperature dependence of the PL ratio of 524 and 545 nm peaks corresponding to  $^4H_{11/2} \rightarrow ^4I_{15/2}$  and  $^4S_{3/2} \rightarrow ^4I_{15/2}$  transitions, respectively.

1. Yuan, H., et al., *Gold nanostars: surfactant-free synthesis, 3D modelling, and two-photon photoluminescence imaging*. Nanotechnology, 2012. **23**(7): p. 075102.
2. Li, Z., et al., *Construction of LRET-Based Nanoprobe Using Upconversion Nanoparticles with Confined Emitters and Bared Surface as Luminophore*. Journal of the American Chemical Society, 2015. **137**(9): p. 3421-3427.